Biosensors and Bioelectronics 24 (2009) 1700–1705

Contents lists available at ScienceDirect

Biosensors and Bioelectronics

journal homepage: www.elsevier.com/locate/bios

Chitosan/polyaniline hybrid conducting biopolymer base impedimetric immunosensor to detect Ochratoxin-A

Raju Khan [a], Marshal Dhayal [b,*]

[a] Analytical Chemistry, North East Institute of Science & Technology, Jorhat 785006, Assam, India
[b] Department of Bio-Engineering, University of Washington, Seattle, USA

ARTICLE INFO

Article history:
Received 12 June 2008
Received in revised form 16 August 2008
Accepted 29 August 2008
Available online 6 September 2008

Keywords:
Polyaniline
Chitosan
Immunosensor
Electrochemical impedance spectroscopy
Ochratoxin-A

ABSTRACT

Chitosan (CS)–polyaniline (PANI) hybrid conducting biopolymer film was obtained on indium–tin-oxide (ITO) electrode using electrochemical polymerization process. Fourier transform infrared (FT-IR) spectra of PANI–CS had showed covalent and hydrogen binding between PANI and CS molecules. Electrochemical impedance spectroscopy (EIS) measurements had showed low charge transfer resistance (R_{CT}) of PANI–CS and PANI. Successive rabbit antibody (IgGs) immobilization on PANI–CS, CS and PANI matrixes surface were confirmed with FT-IR and EIS measurements. Ochratoxin-A (OTA) interaction with IgGs had increased R_{CT} values and showed linear response up to 10 ng/mL OTA concentration in electrolyte. Relative change in R_{CT} was higher in PANI–CS due to higher proportion of carboxylic and hydroxyl functionalities at PANI–CS matrix surfaces. The absolute sensitivity of PANI, CS, and PANI–CS were 16 ± 6, 22 ± 9 and $53 \pm 8\ \Omega$ mL/ng, respectively derived from slope of linear response up to 10 ng/mL with 1 ng/mL minimum detection limit.

1. Introduction

Ochratoxin-A (OTA) is one of a mycotoxin found in food products, human blood, breast milk, tissues and organs of animals (Hult et al., 1982; Zimmerli and Dick, 1995) that can cause several health problems. Therefore several researchers have been working to develop different processes to detect toxic compounds found in several different types of food samples (Ghindilis et al., 1998; Adany et al., 2007; Ngundi et al., 2005; Owino et al., 2007; Piermarini et al., 2007; Micheli et al., 2005; Logrieco et al., 2005). Different types of methods had been used to detect Ochratoxin-A such as liquid chromatography coupled to fluorescence detection (Osnaya et al., 2008; Penas et al., 2004), solid-phase microextraction coupled to liquid chromatography–tandem mass spectrometry (Vatinno et al., 2008), real-time PCR assays (Morello et al., 2007), optical waveguide lightmode spectroscopy technique (Adany et al., 2007) and electrochemical detection (Siontorou et al., 1998). Recently the electrochemical detection method (Wang et al., 2008; Elizalde-Gonzalez et al., 1998) had been most commonly used technique to determine the sensitivity of the toxicity detection because it has a fast response and does not require sample labeling. Simon et al. (2008) had discussed two indirect competitive enzyme-linked immunosorbent assay strategies for OTA electrochemical immunosensors.

In the above-mentioned techniques, an electrochemical analysis emerged as one of the most promising cost effective detection technique with rapid response to detect toxic molecules in electrolytes (Carlson et al., 2000; Fu et al., 2005). Polyaniline (PANI) has been used as a cost effective conducting polymer (MacDiarmid and Epstein, 1994; Kumar et al., 1998; Ahuja et al., 2007) in biosensors from a long time. Biological and electronic properties of PANI were modified by doping different types of inorganic nano-materials (Schultze and Karabalut, 2005). Similarly chitosan (CS) has been also extensively used in biosensors due to its biodegradable, biocompatible and non-toxicity (Luo et al., 2004). Separately both PANI and CS had showed excellent properties as conducting and biocompatible material, respectively for biosensor application. However CS has limited conductivity whereas PANI has limited biocompatibility which has been a subject of intensive research in last decade or so.

There were several attempts to improve the performance of CS and PANI which depends on structural modification and surface chemistry by incorporating nano-metal-oxides (Schultze and Karabalut, 2005; Tan et al., 2005; Feng et al., 2006; Wu et al., 2007; Liu et al., 2005; Khan and Dhayal, 2008a,b). Synthesis of metal nano-particles itself is a very complex process and requires several chemical processes. Therefore the chemicals used for synthesis and non-degradable characteristics of metal oxides can have several environment issues when chemical wastes were disposed.

* Corresponding author. Tel.: +1 206 543 7331; fax: +1 206 685 3300.
E-mail addresses: khan.raju@gmail.com (R. Khan), marshaldhayal@yahoo.com (M. Dhayal).

0956-5663/$ – see front matter © 2008 Elsevier B.V. All rights reserved.
doi:10.1016/j.bios.2008.08.046

Secondly oxidative characteristics of nano-materials can also limit the stability during storage and using electrodes in electrolytes. Considering these points, the interest of this study was to develop a process for metal free conducting biopolymer matrixes which have (i) advantages for technological applications, (ii) having biodegradation property and (iii) is cost effective.

A process had been developed to synthesize hybrid PANI–CS matrix as a metal free biosensor with excellent conducting and biocompatible properties polymer and have biodegradable property. However, the most challenging task was to obtain electrochemically deposited PANI–CS matrix. This was because controling agglomeration of CS molecules in electrolyte requires optimizing several parameters. PANI–CS films were characterized by using different techniques such as scanning electron microscopy (SEM), Fourier transform infrared (FT-IR) and electrochemical impedance spectroscopy (EIS) and application in biosensor has been discussed.

2. Materials and methods

Chitosan (Mw 2.4×10^6), aniline (99.5%) and hydrochloric acid (32%) of analytical grade were purchased from Sigma–Aldrich. CS flakes (0.5 g) were dissolved in 10 mL of 0.05 M acetate buffer solution of pH 6.4 to prepare 20.8 μM solution of CS. Electrochemically polymerization of aniline on ITO electrode was carried out by adding 0.2 M aniline into 1 M HCl solution prepared in 10 mL of de-ionized water. Electrochemically novel CS with PANI films was prepared by adding 0.2 μM CS in 10 mL de-ionized water in 0.2 M aniline solution with 1 M HCl. Chronoamperommetry method was used for PANI and PANI–CS film formation by adjusting potential from −0.2 to 0.9 mV in 150 s. CS films were deposited by spin coating at 500 rpm/s and drying at 50 °C temperature. Film surface areas for sensor were 0.25 cm^2 on indium–tin-oxide (ITO) substrate. Successfully regeneration of ITO substrate was also carried out several times. The CS–PANI films were cleaned with a chemical cleaning process and followed by plasma cleaning.

Rabbit antibody (IgGs) solution was prepared in 50 mM phosphate buffer (PBS) at pH 7 and a 0.15 M NaN_3 was used as a preservative. Freshly prepared 10 μL of IgGs solution was spread on PANI, CS and PANI–CS electrodes for physico-sorption at surface and allowed to dry at 4 °C for 12 h. The IgGs immobilized electrodes were washed with phosphate buffer solution to remove unbounded sites. Bovine serum albumin (BSA; 98% purity) dissolved in PBS was used as the blocking agent. IgGs immobilized electrode were dipped in BSA solution and dried at 4 °C for 6 h. These electrodes were washed again with PBS before using for OTA. Ochratoxin-A from *Aspergillus ochraceus* (*Aspergillus oryzae*) was purchased from Sigma–Aldrich (Cat. No. O1877). OTA solution was prepared by dissolving in PBS with 10% methanol.

For the detection of OTA, IgGs immobilized working electrodes was placed in 10 mL phosphate butter (50 mM, pH 7.0 and 0.9% NaCl) containing $Fe(CN)_6^{3/4-}$ and 20 μL volume with different concentrations of OTA was added by stirring for 30 s before the measurements. Platinum wire and Ag/AgCl were used as counter and reference electrodes, respectively between the frequency ranges 0.01 and 10^5 Hz at constant 5 mV amplitude and 250 mV initial potential for all the measurements.

Autolab Potentiostat/Galvanostat (Eco Chemie, Netherlands) was used for EIS measurements with three-electrode system. FT-IR spectra recorded on PerkinElmer, Spectrum BX II spectrophotometers. The surface morphology of the film was studied using SEM, LEO 440 model and the contact angle was measured with water droplet using sessile drop method in KRUSS DSA10 system.

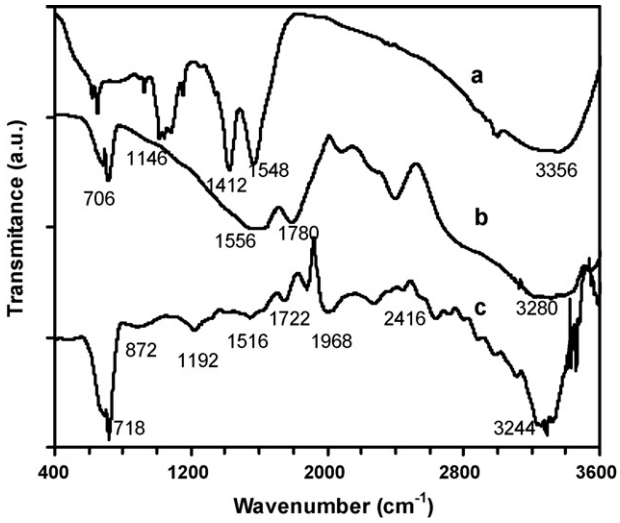

Fig. 1. FT-IR spectra of (a) CS, (b) PANI–CS and (c) PANI.

3. Results and discussion

Fig. 1 showed wide band between 2600 and 3600 cm^{-1} in CS film FT-IR spectrum due to N–H stretching with hydrogen bonded amino groups, free O–H stretching vibration and aliphatic C–H stretching (Nunthanid et al., 2004). Two distinct peaks in spectra at 1548 and 1412 cm^{-1} were observed due to acetylacetonate chelating ligand (Jiang and Zuo, 2001). IR band at 1146 cm^{-1} was due to C–C–N in amines bending and peaks between 922 and 1058 cm^{-1} were due to C–O stretching of CH–OH in cyclic alcohols. Peak at 650 cm^{-1} was due to C–O–H bending in alcohols. Broadening in characteristics peaks associated with PANI and CS was observed in FT-IR spectra of hybrid PANI–CS film. This increase in broadening of IR bands between 2710 and 3600 cm^{-1} was due to covalent and hydrogen binding between $-NH_2$ and –OH groups of PANI and CS, respectively. The IR peak at 1780 cm^{-1} was associated with C=O stretch in $-HNCOCH_3$ arising from pristine chitin (Sung et al., 2003). The increased broadening of bands between 1680 and 1410 cm^{-1} have confirmed covalent binding of acetylacetonate in CS (Jiang and Zuo, 2001) with –NH of primary amide in PANI (Zhang and Wan, 2002). Additional bands in spectra were associated with carboxylic acid due to H-bonded OH stretch of PANI with CS in polymer chain. IR Peak associated with C=O stretch in $-HNCOCH_3$ indicates possibility of agglomeration of CS molecules and was minimized by adjusting pH of CS-based solution for electrochemical polymerization.

FT-IR spectrum of PANI has strong absorption bands at 718 and 872 cm^{-1} due to presence of aromatic ring and possible deformation of C–H vibrations as shown in Fig. 1. Bands between 1192 and 1516 cm^{-1} were associated with C–N in aromatic amines due to C–N stretching. IR band at 1722 cm^{-1} was due to C=C stretching of benzenoid rings and quinoid rings. IR peaks between 1852 and 2416 cm^{-2} were associated with –N≡N in diazonium salts. The IR band at 2610–3252 cm^{-1} correspond to N–H stretching with hydrogen bonded amino groups and free O–H stretching vibration (Zhang and Wan, 2002).

PANI, CS and PANI–CS films surface morphology was observed using SEM and shown in Fig. 2. SEM pictures of PANI and PANI–CS films had showed very good uniformity whereas CS film was not as uniform as PANI. This was because PANI and PANI–CS films were obtained by electrochemical polymerization whereas only CS films were deposited by spin coating. Electrochemical polymerization of only CS had agglomeration in electrolyte solution; hence, using CS

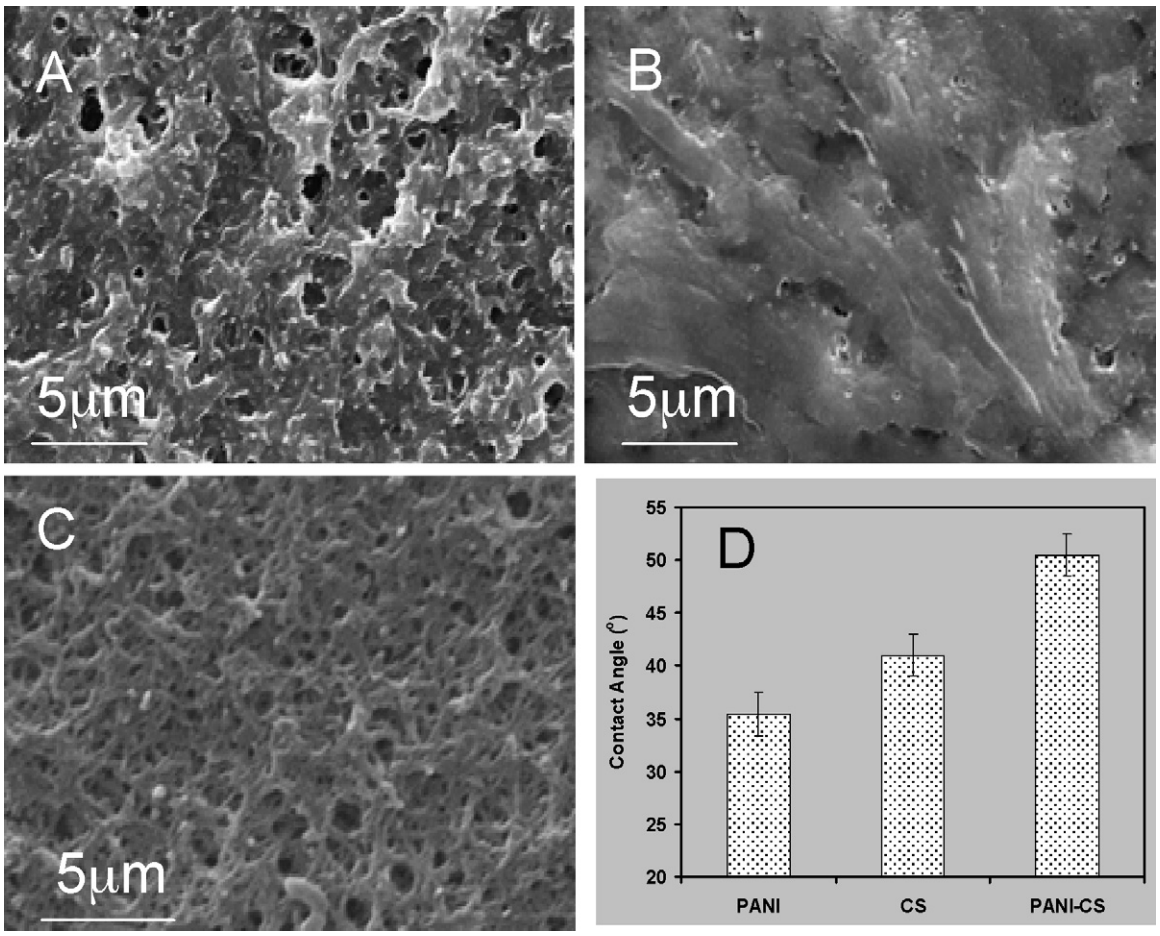

Fig. 2. Scanning microscopic picture of (A) PANI (B) CS (C) PANI–CS and (D) contact angle measurements.

films for immnunosensor as a control condition were deposited by a spin coating process. Addition of CS in PANI had improved both uniformity and porosity in PANI–CS films.

Contact angles for the three different types of films were measured and shown in Fig. 2D. PANI–CS film had higher hydrophobic characteristics relative to only CS and PANI. Controlling both surface morphology and the chemistry of matrix were important to immobilize bio-molecules to achieve higher sensitivity of sensor. These were two independent variables because higher –OH functional group on the surface has a lower contact angle. This correlation was possible only when all other parameters such as surface morphology, porosity and chemical nature of the film were the same. In this study, all these matrixes had different chemical characteristics and SEM observation had showed a significant difference in surface morphology. Therefore, the relative change in contact angle was not directly linked with the hydroxyl group but was associated with per unit area adhesion energy. That energy expression can be derived from Young–Dupre equation $\Upsilon(1+\cos\theta)$; where Υ is surface tension and θ is contact angle. Therefore when $\theta < 90^\circ$ (was case in this study), change in contact angle was possibly dominated by relative change in surface morphology.

EIS response of PANI, CS and PANI–CS films were obtained at different potential and the relative change in R_p as a function of applied potential was studied as shown in Fig. 3. Owino et al. (2007) had also reported EIS measurements at various potential and this process was used to investigate the effect of surface charge modulation on the electrodes surface. PANI–CS film had higher stability against modulated surface charges.

Both Nyquist and Bode (see supplement information for Bode plots) plots were obtained and used to determined relative change in surface-charge resistance at zero potential. Interfacial R_{CT} and C_d in Nyquist plot of impedance were obtained from real (Z') and imaginary ($-Z''$) impedance at different frequencies using the following equation (Bard and Faulkner, 2000) for a parallel RC circuit.

$$Z(\omega) = Z' + jZ'' = R_s + \frac{R_p}{(1 + j\omega C_d)} \quad (1)$$

$$Z' = R_s + \frac{R_p}{1 + \omega^2 R_p^2 C_d^2} \quad \text{and} \quad -Z'' = \frac{\omega R_p^2 C_d}{1 + \omega^2 R_p^2 C_d^2} \quad (2)$$

where, R_s was the electrolyte solution resistance and R_p was polarization resistance. R_p obtained at zero potential was described as surface-charge resistance (R_{CT}). The frequency associated with maximum Z'' and R_{CT} were used to calculate C_d using the following equation.

$$R_{CT} C_d = \frac{1}{2\pi f_{max}} \quad (3)$$

Warburg resistance (Z_w) was also obtained in Nyquist plot and an equivalent circuit to describe the electrical response at electrode shown in Fig. 4A. In the plot Warburg impedance was expressed by an intercept of straight line having a slope of unity (Bard and Faulkner, 2000) and can be derived from the following equation:

$$Z_w(\omega) = W_{int} + \left(\frac{R_p \lambda}{\sqrt{2\omega}}\right)[1 - j] \quad (4)$$

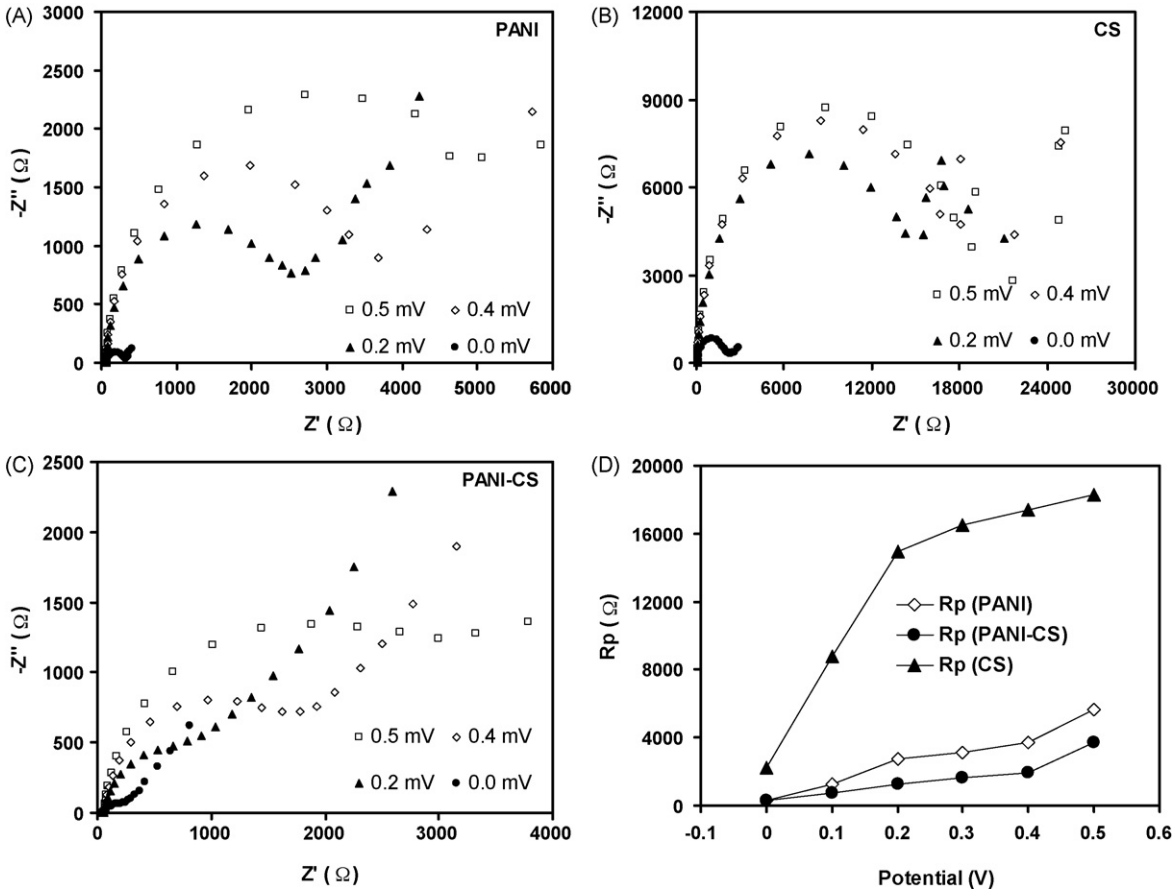

Fig. 3. Nyquist plots at different potentials (A) PANI, (B) CS, (C) PANI–CS and (D) charge transfer resistance (R_{CT}) for PANI, PANI–CS and CS at different potentials.

$$W_{int} = R_s + R_p - R_p^2\lambda^2 C_d \quad (5)$$

where $\lambda = (k_f/\sqrt{D_O} + k_b/\sqrt{D_R})$, k_f and k_b were forward and backward electron-transfer rate constants, D_O and D_R were the diffusion coefficient of oxidant and reductant. R_s and $R_s + R_{CT}$ values were obtained from standard commercial software available with the instrument and were also separately calculated from the semicircle and straight line fitting in excel spreadsheet. Table with all the values were given in the supplement information. Similar information was also obtained from Bode diagram of impedance and phase shift with frequency (see supplement information).

Warburg impedance of CS film had resistive (slope of strait line was <45°) characteristics similar to other reported EIS measurement (Luo et al., 2005). Whereas expected PANI films had capacitive characteristics at the interface. Previously electrochemical impedance of various oxidation states of polyaniline films were also studied (Cho et al., 1996) and capacitive characteristics at the interface was controlled by changing the oxidation state of PANI. Hybrid PANI–CS matrix had showed capacitive characteristic at the interface with low R_{CT} value. Experimentally obtained low value of R_{CT} in PANI–CS can be explained as (i) existence of cationic

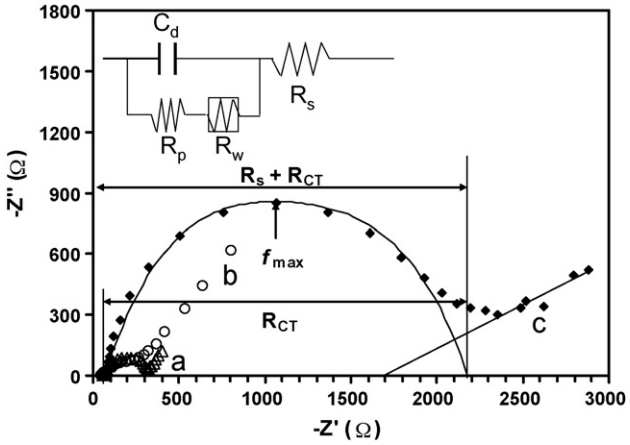

Fig. 4. EIS Nyquist plots of PANI, CS and PANI–CS.

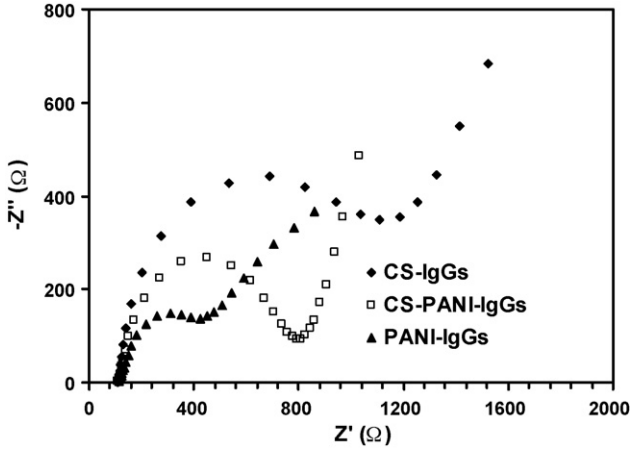

Fig. 5. EIS Nyquist plots of rabbit antibody and BSA immobilized PANI, CS and PANI–CS.

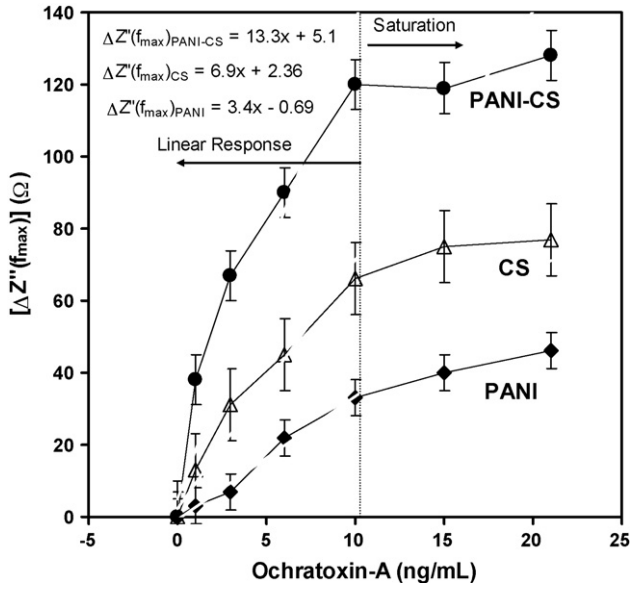

Fig. 6. Relative sensitivity (%) of PANI, PANI–CS and CS with different concentration of OTA.

ions on CS molecules could diffuse into PANI molecules to change oxidation state, and (ii) this diffusion process can increase the conductivity and hence compensate higher resistance of CS due to large molecules size.

Successive immobilization of IgGs had increased R_{CT} values of PANI and PANI–CS electrodes as shown in Fig. 5. Slope of the straight line associated with Warburg impedance also increased after IgGs was immobilized. Two semi-circles (can also be realized from phase shift Bode plot, shown in supplementary information) were seen on PANI films after IgGs immobilization which indicated two distinct characteristics of PANI and IgGs. Huang et al. (2006) had successively demonstrated the use of electrochemical impedance spectroscopy for monitoring allergen–antibody reactions with a metal surface. Therefore this observed change in R_{CT} after IgGs immobilization was due to dielectric and insulating features at the electrodes electrolyte interface and was associated with successive immobilization of antibodies.

Hybrid PANI–CS matrixs practical application for an immunosensor was demonstrated by detecting OTA in electrolyte on IgGs immobilized electrodes. IgGs immobilized electrodes were placed in 10 mL phosphate butter (50 mM, pH 7.0 and 0.9% NaCl) containing $Fe(CN)_6^{3/4-}$ and subsequently different concentrations (1, 2, 3, 4, 5 and 6 ng/mL) of OTA were added by stirring for 30 s, before each measurement was taken. Relative change in surface charge transfer resistance was observed at different concentrations of OTA in electrolyte for all three matrixes (see supplement information for EIS spectra). The interaction of OTA with IgGs on the electrodes surface had significantly changed both R_{CT} and C_d.

Reproducibility of EIS spectra was studied by two different methods: (i) EIS spectra were repeated several times on the same film surface in electrolyte and (ii) different films were prepared from the same stock solution. In both cases good reproducibility were observed. However, reproducibility of absolute value of data obtained on the film surfaces prepared from different stock solutions had about 20–30% deviation. This error limit was calculated base on relative change in R_{CT}. This large variation was possibly associated with a change in the probe surface area, film thickness and change in the electrolyte concentration. However this error limit can be easily minimized for real analytical work by using soft lithography and well controlled automated film deposition process to precisely control surface areas and film thickness, respectively.

For sensing application relative change in EIS spectra have more significant information and very good reproducibility was observed on relative change in EIS spectra after normalizing with initial R_{CT} values. However, relative change in R_{CT} to describe sensitivity of the immunosensor in linear response region had good reproducibility after normalizing values of R_{CT} with controlled condition. Hence, sensitivity of the immunosensor was determined with relative change in $-Z''(w)$ at f_{max} using the following equation.

$$\text{Relative sensitivity (RS\%)} = 100\frac{Z''_{fmax}(x) - Z''_{fmax}(0)}{Z''_{fmax}(0)} \quad (6)$$

where, $Z''_{fmax}(x)$ and $Z''_{fmax}(0)$ were imaginary impedance values for 0 and '*x*' ng/mL concentration of OTA in electrolyte at f_{max} (see supplement information for f_{max} and $Z''_{fmax}(x)$ at different concentration of OTA in electrolyte). Fig. 6 shows RS (%) for CS, PANI and PANI–CS matrixes, which was increased linearly up to 10 ng/mL concentration of OTA and was reached on saturation for further increase. The absolute sensitivity of PANI, CS, and PANI–CS were 16 ± 6, 22 ± 9 and 53 ± 8 Ω mL/ng; respectively derived from slope of linear response up to 10 ng/mL. The interaction of OTA with immunosensor depended on the relative proportion and the activities of IgGs molecules at the surface. PANI–CS matrix had the highest sensitivity relative to PANI and CS. This was due to higher proportion of carboxylic and hydroxyl groups on PANI–CS matrix which had supported IgGs immobilization and activity.

4. Conclusions

Addition of CS in PANI for electrochemical film deposition had enhanced surface morphology on the PANI–CS surface. R_{CT} of PANI–CS film was reduced by one order relative to only CS. The diffusion process at the interface of PANI and PANI–CS films surface had capacitive characteristic. Successive immobilization of IgGs on PANI and PANI–CS electrodes had increased R_{CT} values. Relative sensitivity (%) for CS, PANI and PANI–CS matrixes, were increased linearly up to 10 ng/mL concentration of OTA and reached on saturation for further increase. The RS (%) value indicated that observed relative sensitivity of PANI–CS matrix was about two and three times of only CS and only PANI, respectively.

Acknowledgments

Dr. Raju Khan thanks the Department of Science and Technology (DST, Government of India) for financial support under the Young Scientist project SR/FTP/CS-77/2007. We are grateful to Dr. Vikram Kumar (Director, NPL) for infrastructure support.

Appendix A. Supplementary data

Supplementary data associated with this article can be found, in the online version, at doi:10.1016/j.bios.2008.08.046.

References

Adany, N., Levkovets, I.A., Rodriguez-Gil, S., Ronald, A., Varadi, M., Szendro, I., 2007. Biosensor and Bioelectronics 22, 797–802.
Ahuja, T., Mir, I.A., Kumar, D., Rajesh, 2007. Biomaterials 28, 791–805.
Bard, A.J., Faulkner, L.R., 2000. Electrochemical Methods. Wiley & Sons, New York.
Carlson, M.A., Bargeron, C.B., Benson, R.C., Fraser, A.B., Philips, T.E., Velky, J.T., Groopman, J.D., Strickland, P.T., Ko, H.W., 2000. Biosensors and Bioelectronics 14, 841–848.
Cho, J.H., Lee, H.K., Ryu, K.S., Yo, C.H., Jeong, S.K., Suh, J.S., Oh, E.J., 1996. Molecular Crystals and Liquid Crystals 280, 205–210.
Elizalde-Gonzalez, M.P., Mattusch, J., Wennrich, R., 1998. Journal of Chromatography A 828, 439–444.

Feng, K.J., Yang, Y.H., Wang, Z.J., Jiang, J.H., Shen, G.L., Yu, R.Q., 2006. Talanta 70, 561–565.
Fu, Y., Yuan, R., Tang, D., Chai, Y., Xu, L., 2005. Colloids and Surfaces B: Biointerfaces 40, 61–66.
Ghindilis, A.L., Atanasov, P., Wilkins, M., Wilkins, E., 1998. Biosensor and Bioelectronics 13, 113–131.
Huang, H., Liu, Z., Yang, X., 2006. Analytical Biochemistry 356 (2), 208–214.
Hult, K., Plestina, R., Novak, V.H., Radic, B., Ceovic, S., 1982. Archives of Toxicology 51 (4), 313–321.
Jiang, Z., Zuo, Y., 2001. Analytical Chemistry 73, 686–688.
Khan, R., Dhayal, M., 2008a. Electrochemistry Communication 10 (2), 263–267.
Khan, R., Dhayal, M., 2008b. Electrochemistry Communication 10 (3), 492–495.
Kumar, A., Welsh, D.M., Morvant, M.C., Piroux, F., Abboud, K.A., Reynolds, J.R., 1998. Chemistry of Materials 10, 896–902.
Liu, Y.L., Yang, Y.H., Yang, H.F., Liu, Z.M., Shen, G.L., Yu, R.Q., 2005. Journal of Inorganic Biochemistry 99, 2046–2053.
Logrieco, A., Arrigan, D.W.M., Brengel-Pesce, K., Siciliano, P., Tothill, I., 2005. Food Additives and Contaminants 22 (4), 335–344.
Luo, X.L., Xu, J.J., Du, Y., Chen, H.Y., 2004. Analytical Biochemistry 334, 284–289.
Luo, X.L., Xu, J.J., Zhang, Q., Yang, G.J., Chen, H.Y., 2005. Biosensors and Bioelectronics 21 (1), 190–196.
MacDiarmid, A.G., Epstein, A.J., 1994. Synthetic Metals 65, 103–116.
Micheli, L., Grecco, R., Badea, M., Moscone, D., Palleschi, G., 2005. Biosensor and Bioelectronics 21, 588–596.
Morello, L.G., Sartori, D., Martinez, AldO., Vieira, M.L.C., Taniwaki, M.H., Fungaro, M.H.P., 2007. International Journal of Food Microbiology 119, 270–276.
Ngundi, M.M., Shriver-Lake, L.C., Moore, M.H., Lassman, M.E., Ligler, F.S., Taitt, C.R., 2005. Analytical Chemistry 77, 148–154.
Nunthanid, J., Laungtana-Anan, M., Sriamornsak, P., Limmatvapirat, S., Puttipipatkhachorn, S., Lim, L.Y., 2004. Journal of Controlled Release 99, 15–26.
Osnaya, L.G., Soriano, J.M., Molto, J.C., Manes, J., 2008. Food Chemistry 108, 272–276.
Owino, J.H.O., Ignaszak, A., Al-Ahmed, A., Baker, P.G.L., Alemu, H., Ngila, J.C., Iwuoha, E.I., 2007. Analytical and Bioanalytical Chemistry 388, 1069–1074.
Penas, E.G., Leache, C., Viscarret, M., Obanos, APd., Araguas, C., Cerain, Ald., 2004. Journal of Chromatography A 1025, 163–168.
Piermarini, S., Micheli, L., Ammida, N.H.S., Palleschi, G., Moscone, D., 2007. Biosensor and Bioelectronics 22, 1434–1440.
Schultze, J.W., Karabalut, H., 2005. Electrochimica Acta 50, 1739–1743.
Simon, B.P., Campas, M., Marty, J.L., Noguer, T., 2008. Biosensors and Bioelectronics 23, 995–1002.
Siontorou, C.G., Nikolelis, D.P., Miernik, A., Krull, U.J., 1998. Electrochimica Acta 43, 3611–3617.
Sung, J.H., Choi, H.J., Jhon, M.S., 2003. Materials Chemistry and Physics 77, 778–783.
Tan, X., Li, M., Cai, P., Luo, L., Zou, X., 2005. Analytical Biochemistry 337, 111–120.
Vatinno, R., Vuckovic, D., Zambonin, C.G., Pawliszyn, J., 2008. Journal of Chromatography A. 1201 (2), 215–221.
Wang, H., Meng, S., Guo, K., Liu, Y., Yang, P., Zhong, W., Liu, B., 2008. Electrochemistry Communication 10 (3), 447–450.
Wu, B.Y., Hou, S.H., Yin, F., Li, J., Zhao, Z.X., Huang, J.D., Chen, Q., 2007. Biosensor and Bioelectronics 22, 838–844.
Zhang, Z., Wan, M., 2002. Synthetic Metals 128, 83–89.
Zimmerli, B., Dick, R., 1995. Journal of Chromatography B: Biomedical Sciences and Applications 666 (1), 85–99.